Improvement Power System Dynamic Stability by Using UPFC with Practical Constraints

M. Maleki rizi[1]; S. Abazari[2,*]; N. Mahdian[3]

1- Department of Engineering, Shahrekord University, Shahrekord, Iran.
2- Department of Engineering, Shahrekord University, Shahrekord, Iran, Email: Abazari-s@eng.sku.ac.ir
3- Shahid Rajaie Teacher Training University, Tehran, Iran
*Corresponding Author
Received: 2020-07-26
Revised: 2020-12-15
Accepted: 2021-02-13

Abstract This paper presents enhancement of power system dynamic stability by using unified power flow controller with assuming several real conditions and practical power system constraints. In control method design, we used all four UPFC basic controllers simultaneously with reducing conflict of them by compromising between its control variables. Optimization problem have been used with regarding some constraints of the system and unified power flow controller. Particle swarm optimization algorithm has used to optimize power oscillation damping based on unified power flow controller with an objective function. Simulation results in several multi-machine test power systems demonstrate the capability of applied control system with regarding many constraints and limits of power system and UPFC in different scenarios.

Keywords: Dynamic stability, unified power flow controller, practical constraints, optimization, multi-machine power system.

1. Introduction

Electric power demand increase, bounds the power systems to stress conditions, and leads to undesirable system parameters. To have secure operation of power systems, damping of power system oscillations have attracted a great deal of attention in power-system stability studies. New FACTS devices can be effective in controlling power flow and damping power system oscillations and may use to increase power system operation's flexibility and controllability, to enhance system stability and to achieve better utilization of existing power systems. UPFC is the most important and comprehensive device and has capability of regulating active and reactive power flow and stability improvement in power system. UPFC consists of two converters coupled through a common DC link large capacitor. UPFC is able to control, selectively or simultaneously, transmission network bus-voltage, line impendence or alternatively, the real and reactive power flow in the line by means of series voltage-vector injection. The UPFC can also provide controllable shunt reactive compensation independently. These duties fulfil with to converter voltage magnitude and phase angle control that commonly used PI control.

In inter-area modes, PSS may not produce enough damping, But UPFC is as an interesting approach to help to overcome several power system operating difficulties and controlling voltages at critical buses, transient stabilization and small signal and dynamic control and consequently the overall stability of power systems [1].

UPFC employing a feedback supplementary controller can not only considerably enhance system. It can enhance damping effect in inter-area oscillations and thus these are advantageous over PSSs [2]. Damping effect of UPFC based POD with PSS have compared and better result of UPFC based one is resulted too [3]. To investigate UPFC damping effect, LQR and UPFC control effects on dynamic stability improvement in SMIB had compared [4]. A fuzzy method had used to tune series inverter PI controllers in two-area power system and tended to decrease in oscillation of active power [5]. PSO technique have been used in two PI tanning of UPFC in three-machine power system, to reduce settling time too [6]. To UPFC POD controller design in MMPS, in three-machine system, with selecting damping ratio based objective function LQR have used under different loading condition and better result demonstrated [7]. Many researchers use PSO for this application and some of them used adaptive PSO to improve damping controller results in compare with standard PSO and some other previous PSO types[1]. IGWO had compared with DE and PSO to optimize UPFC POD controller with ITAE criteria too and demonstrated stability enhancement of MMPS in three-machine system while comparing using only m_B or δ_E [8]. Several researches have tried to use improved approaches of PSO to enhance oscillation damping of power system such as [9], which try to optimize system energy function using UPFC while only using two basic controllers of UPFC in three-machine reduced power system model. Already Comparison and Assessment of Conventional and Optimal Coordinated PSS and UPFC Damping Controller for SMIB system in SIMULINK platform, regarding overshoot and settling time simulated

[10]. And stability enhancement of a three machine system by using the coordinated application of the UPFC and the PSS designed by using the Firefly algorithm and was compared with Genetic search algorithm approach too [11]. Synchronized use of PSS along with UPFC can result in further improvement in reliability, controllability and mitigation of power system oscillations thus further improving the system stability. using the evolutionary Cuckoo algorithm technique for transient stability enhancement of two machine power system, through coordinated design of SS and UPFC in SIMULINK platform had examined too[12]. Recently researchers, try to use some of nonlinear control methods to control UPFC in single or multi machines power system so in [13] we can see using multi input back stepping in multi-machine power system equipped with UPFC oscillation damping control.

In most previous researches to investigate UPFC dynamic stability enhancement, they have not used all basic controllers together and simultaneously and they have not considered any practical limitation of power network in these regulators adjustment too. If we don't consider the network limitations, it is possible that in spite of achieving good damping and dynamic result, in real condition we can't use UPFC in those conditions, because some limitations such as line thermal limits can cause damage to system or instability in real conditions.

Here, beside of using optimized POD controller with Particle Swarm Optimization (PSO) algorithm, we have used model of UPFC in multi-machine power system (MMPS) to investigate dynamic stability with regarding many constraints of power system such as line transmission capacity limits in both steady state UPFC calculations and small signal oscillations. Another important constraint which we assumed while adjusting power flow in line is rating limits of the UPFC because in real condition the rating of devices and economic conditions seriously limits these ratings. We will deal with UPFC in the following section.
In many of those researches multi machine system only simulated by SIMULINK and multi machine study restricted only to three- machine or two-area system.

In the next section UPFC introduced. In section 3 and 4 basic control and supplementary control of UPFC presented. After introducing PSO in section 5, in section 6 steady state and dynamic equations of power system with UPFC installed described. Finally in section 7 results of this study demonstrated.

2. Unified power flow controller

The UPFC consists of a boosting transformer and an excitation transformer linked by two back-to-back converters. Figure 1 shows UPFC in power system. Equation 1 expresses the UPFC terminals voltage relation with dc link voltage and UPFC parameters.

$$\overline{\boldsymbol{V}}_{\boldsymbol{E}}=\frac{m_E Vdc}{2}e^{j\delta_E}, \quad \overline{\boldsymbol{V}}_{\boldsymbol{B}}=\frac{m_B Vdc}{2}e^{j\delta_B} \tag{1}$$

The series branch of the UPFC injects an AC voltage, Where, m_B is pulse width modulation of series (boosting) converter. By m_B controlling, the magnitude of series injected voltage can be control. m_E is pulse width modulation of shunt (exciting) inverter. By m_E controlling, the output voltage of the shunt converter is controlling. δ_B is phase angle of series injected voltage. δ_E is voltage phase angle of the shunt inverter.

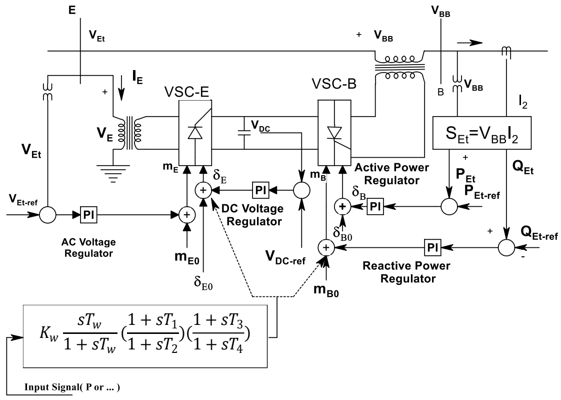

Fig. 1. UPFC in power system

with controllable magnitude and phase angle at the power frequency [2]. And then can exchange real and reactive power with installed line. The shunt converter has used primarily to provide active power demand of the series converter through a common DC link and can exchange reactive power to adjust voltage of bus, which is connected. Then UPFC is a combination of STATCOM and SSSC.

The comprehensive models of UPFC for steady state, transient stability and dynamic stability studies and also dynamic model of the system installed with UPFC is presented in [14]. Wang et al have proposed a unified model of a multi-machine power system and developed two UPFC models, which have been linearalized and incorporated into the Phillips-Heffron model [14]. We have used the comprehensive UPFC model, which is more complete for steady state analysis and applicable in power flow solution.

3. UPFC basic control

Figure 1 shows the UPFC power and control flow diagram. As we can see, by adjusting the magnitude and phase angle of the shunt (exciting) converter, bus voltage and dc voltage across common capacitor will be controlled. Shunt active and reactive power exchange is related with active power which series converter request and bus voltage requirements to be kept in accepted value respectively. Active and reactive power flow can be controlled by adjusting magnitude and phase angle of series converter. Wang showed that parameters of UPFC i.e. $\boldsymbol{m_E}$, $\boldsymbol{m_B}$, $\boldsymbol{\delta_E}$ and $\boldsymbol{\delta_B}$ should be modulated to achieving desired damping of oscillation too. Equations 2 to 5 express these 4 basic control functions. Wang et al investigated the control conflict between UPFC multiple control functions and their interactions in single-machine infinite -bus system and showed that sometimes using all four control function may decrease accuracy of results [15]. Then their adjustment with attention to this interaction is very important. We used all of these four controllers simultaneously and have done compromise between four control variables.

$$\boldsymbol{\delta_B} = \left(\frac{1}{1+T_{\delta B}s}\right)\left(K_{Pp} + \frac{K_{Pi}}{s}\right)\left(P_{Ref} - P\right) \quad (2)$$

$$m_B = \left(\frac{1}{1+T_{mB}s}\right)\left(K_{Qp} + \frac{K_{Qi}}{s}\right)\left(Q_{Ref} - Q\right) \quad (3)$$

$$m_E = \left(\frac{1}{1+T_{mE}s}\right)\left(K_{Vp} + \frac{K_{Vi}}{s}\right)\left(V_{Ref} - V\right) \quad (4)$$

$$\delta_E = \left(\frac{1}{1+T_{\delta E}s}\right)\left(K_{DCp} + \frac{K_{DCi}}{s}\right)\left(V_{DC,Ref} - V_{DC}\right) \quad (5)$$

where $\boldsymbol{T_x}$ are delay time constants, and $\boldsymbol{K_{xp}}$ and $\boldsymbol{K_{xi}}$ are PI controllers proportional and integral gains respectively. P, Q, V and $\boldsymbol{V_{DC}}$ are active and reactive power flow through line and bus voltage which UPFC is connected and UPFC dc link voltage respectively.

The main practical restriction that we want to apply to system is real and reactive power limits which UPFC can supply without any external power supply. Due to technical and economic restriction the rating of UPFC power is limited and this leads to applying limits of real and reactive power by additional limiter blocks and then modifying the UPFC related parameters in each iteration.

4. Power oscillation damping controller based on UPFC

Secondary control design has known as the damping controller design, which is a supplementary control loop that is designed to enhance transient stability of entire electric power system. The adverse interaction between PSS and series part control have compensated by providing UPFC based damping controller. Thus this is another important reason of UPFC POD controller improvement and its application beside basic controls.

Commonly the POD controllers have a transfer function consisting of Gain, a washout function and two lead-lag blocks. It is showed that the UPFC based POD controller works effectively in single machine system. To improve its dynamic performance in a multi-machine system, the behaviour of the controllers must be coordinated [16]. In [17] the speed deviation is selected and all four parameters of UPFC tried to be output of POD. And resulted that $\boldsymbol{m_B}$is the best selection. In this paper the active power of transmission line which UPFC controls its power flow is used as input signal and we have used this input and output. POD controller consists of $\boldsymbol{T_W}$ wash-out time constant which selected constant and K wash-out gain and $\boldsymbol{T_1}$to $\boldsymbol{T_4}$ lead-lag time constants which should be adjust.

Fixed parameter classical controller is not suitable for the UPFC damping control design. Then, a flexible controller should develop. Several approaches proposed for it, such as root locus and sensitivity analysis, pole placement, and robust control. The conventional techniques require heavy computation and slow convergence. And the search methods may be trapped in local minimum and the solution obtained may not be optimum. In addition, it is necessary that the designed controller provide some robustness to the variations of parameters, conditions, and configurations. Also the controller parameters which stabilize the system in a certain operating condition may no longer have acceptable results in case of large disturbances [17].

We can use an optimization problem, base on Eigen values multi-objective function reflecting the combination of damping factor and damping ratio is considered as:

$$J = \sum_{j=1}^{NP} \sum_{\sigma_i \geq \sigma_0} \left(\sigma_0 - \sigma_{ij}\right)^2 + \alpha \sum_{j=1}^{NP} \sum_{\zeta_i \geq \zeta_0} \left(\zeta_0 - \zeta_{ij}\right)^2$$

$$\boldsymbol{f(x)} = \mathbf{min}\,\boldsymbol{J} \qquad \begin{array}{l} K^{\min} \le K \le K^{\max} \\ T_1^{\min} \le T_1 \le T_1^{\max} \\ T_2^{\min} \le T_2 \le T_2^{\max} \\ T_3^{\min} \le T_3 \le T_3^{\max} \\ T_4^{\min} \le T_4 \le T_4^{\max} \end{array}$$

(6)

where $\boldsymbol{\sigma_{ij}}$ are real parts of system Eigen values and $\boldsymbol{\sigma_0}$ is desired real part of Eigen value, $\zeta_{\boldsymbol{ij}}$ are damping ratios of system variables and $\zeta_{\boldsymbol{0}}$ is desired damping ratio. Both real part and damping ratio are important in system stability then the objective function consists of two parts which each part related to each of these two main factors and α is the constant coefficient which determine the importance weight of the two parts of the objective function. This optimization problem can solve with one of analytical or numerical techniques. Here we have used PSO which introduced briefly in next section.

5. Particle swarm optimization algorithm

PSO is an optimization technique which is population-based introduced by Kennedy and Eberhart to solve the optimization problem with constraint. In PSO system, multiple solutions are candidate and collaborate simultaneously. Each candidate, called a particle, flies in the problem search space looking to land on the optimal position. Particles, during the generations, adjusts their own positions according to theirs own experience and the experience of neighbour particles. This algorithm combines global and local search methods, and tries to balance exploitation and exploration. In this technique new velocity and position of each particle will be updated according to the following equations [18]:

$$\begin{aligned} V_i[k+1] &= w \times V_i[k] + c_1 \times r_1 \times \left(pbest_i[k] - X_i[k]\right) \\ &+ c_2 \times r_2 \times \left(gbest[k] - X_i[k]\right) \quad , \quad i = 1,2,\cdots,N \end{aligned} \quad (7)$$

$$X_i[k+1] = X_i[k] + V_i[k+1] \quad (8)$$

where N is number of particles, k is the current iteration, $\boldsymbol{w}$ is an inertia weight, $\boldsymbol{r_1}$ and $\boldsymbol{r_2}$ are random variables between 0 and 1, $\boldsymbol{c_1}$ and $\boldsymbol{c_2}$are acceleration coefficients. $\boldsymbol{V_i}$ and $\boldsymbol{X_i}$are the velocity and position of the particle $\boldsymbol{i}$ respectively. $\boldsymbol{pbest_i}$ is the local best position of particle $\boldsymbol{i}$. gbest is the global- best position of all particles.

To optimize J function that mentioned above with PSO the lead-lag controller parameters; $\boldsymbol{T_1}$ to $\boldsymbol{T_4}$ and wash-out gain K are adjusted. The UPFC modeling together with power system have dealt in next section.

6. Modelling and control of power system with UPFC installed

Figure 2 shows the UPFC in multi-machine power system. Performance analysis and control functions synthesis of UPFC require its steady state and dynamic models. In order to simulate the multi-machine power system that contains a UPFC, the UPFC have modelled for both steady state and dynamic operations condition.

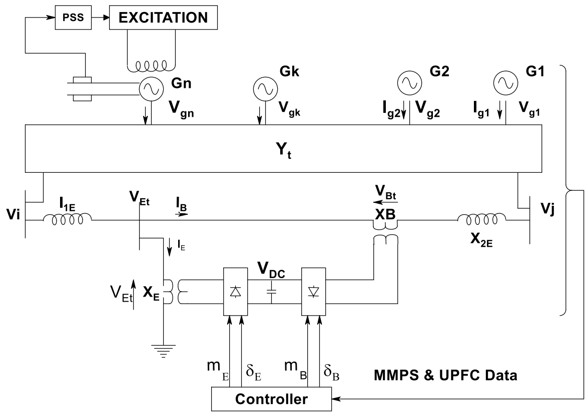

Fig. 2. UPFC in multi-machine power system

6.1. Power system with UPFC steady state model

The basic control strategy is such that the shunt converter of the UPFC controls the UPFC bus voltage, shunt reactive power and the dc link capacitor voltage. The series converter controls the transmission line real and reactive power flow. Then the steady state model assumes that the UPFC is operating to keep real and reactive power flows at the receiving bus and to regulate sending bus voltage magnitude. Thus a two-source UPFC steady-state model including source impedances has proposed in [19].

This UPFC model is extension of the power flow equations and, hence, it is suitable for incorporation into an existing Newton-Raphson load flow algorithm. In this unified solution, the UPFC state variables have adjusted simultaneously with the nodal network state variables. Hence, the interaction between the network and the UPFC has taken in to account.

These steady state parameters values will use to calculate and determine base values of UPFC control parameters. This load flow implementation can help to select proper placement of UPFC.

With reducing bus admittance matrices to generator internal buses and UPFC terminal bus the following equation can be write:

$$\bar{Y} = \begin{bmatrix} Y_{GG} & Y_{GU} \\ Y_{UG} & Y_{UU} \end{bmatrix}, \bar{E} = \begin{bmatrix} \bar{E}_G \\ \bar{V}_U \end{bmatrix}, \bar{I} = \begin{bmatrix} \bar{I}_G \\ \bar{I}_U \end{bmatrix}, \quad \boldsymbol{\bar{Y}\bar{E} = \bar{I}} \tag{9}$$

While, $\boldsymbol{Y_{GG}}$ is reduced admittance matrices connecting the generator current injection to the internal generator voltages. $\boldsymbol{Y_{GU}}$ is admittance matrices component which gives the generator currents due to the voltages at UPFC buses. $\boldsymbol{Y_{UG}}$ is admittance matrices component which gives UPFC currents in terms of the generator internal voltages. $\boldsymbol{Y_{UU}}$ is admittance matrices connecting UPFC currents to the voltages at UPFC buses. $\boldsymbol{\bar{E}_G}$ is vector of generator internal bus voltages. $\boldsymbol{\bar{V}_U}$ is vector of UPFC ac bus voltages. $\boldsymbol{\bar{I}_G}$ is vector of generator current injections. $\boldsymbol{\bar{I}_U}$ is vector of UPFC currents injected to the power network. Then, these parameters instant values will incorporate in deriving matrices equation of multi machine power system with UPFC installed which is essential in dynamic stability analysis.

6.2. Power system linearzed model

Traditionally, for the small signal stability studies of power system, the linear model of Phillips-Heffron has used, and has provides reliable results [20]. Although the model is linearized, it is enough accurate for studying low frequency oscillations and dynamic stability of power systems. The dynamic model of the system completely presented in [20]. The injection model has used to dynamic stability control of UPFC in MMPS modelling too [4]. The nonlinear dynamic model of the system installed with UPFC has given as (10)-(14). Equation (14) shows the UPFC dynamics.

$$\dot{\delta}_i = \omega_b(\omega_i - 1) \tag{10}$$

$$\dot{\omega}_i = \frac{(P_{mi} - P_{ei} - D_i\omega_i)}{M_i} \tag{11}$$

$$\dot{E}'_{qi} = \frac{(-E'_{qi} + E_{fdi})}{T'_{doi}} \tag{12}$$

$$\dot{E}_{fdi} = \frac{(-E_{fdi} - K_{ai}(V_{Ref} - V_t))}{T_{ai}} \tag{13}$$

$$\mathbf{\dot{V}_{DC} = \frac{3m_E}{4C_{dc}}\left(\sin\delta_E I_{Ed} + \cos\delta_E I_{Eq}\right) + \frac{3m_B}{4C_{dc}}(\sin\delta_B I_{Bd} + \cos\delta_B I_{Bq}} \tag{14}$$

where, i=1, 2, 3,…, n (the generators 1 to n), $\boldsymbol{\delta_i}$ is rotor angle of ith generator, $\boldsymbol{\omega_i}$ is rotor speed of ith generator, $\boldsymbol{P_{mi}}$ is mechanical input power of ith generator, $\boldsymbol{P_{ei}}$ is electrical output power of ith generator, $\boldsymbol{E'_{qi}}$ is internal voltage behind $\boldsymbol{x'}$ of ith generator, $\boldsymbol{E_{fdi}}$ is equivalent excitation voltage of ith generator, $\boldsymbol{T_{ei}}$ is electric torque of ith generator, $\boldsymbol{T'_{doi}}$ is time constant of excitation circuit of ith generator, $\boldsymbol{K_{ai}}$ is regulator gain of ith generator, $\boldsymbol{T_{ai}}$ is regulator time constant of ith generator, is $\boldsymbol{V_{tRefi}}$ is reference voltage of ith generator and $\boldsymbol{V_t}$ is terminal voltage. And:

$$P_e = V_{TD}I_d + V_{TQ}I_q \tag{15}$$

$$V_{TD} = X_Q I_q \tag{16}$$

$$V_{TQ} = E'_q - X_D{}' I_d \tag{17}$$

$$V_{Ti} = \sqrt{V_{TDi}^2 + V_{TQi}^2} \tag{18}$$

Where:

$$\boldsymbol{\omega} = [\,\omega_1\ \omega_2 \dots\ \omega_n]^T, \quad \boldsymbol{E'_q} = \left[\,E'_{q1}\ E'_{q2} \dots\ E'_{qn}\right]^T$$

$$\boldsymbol{E_{fd}} = \left[\,E_{fd1}\ E_{fd2} \dots\ E_{fdn}\right]^T$$

$$\boldsymbol{V_{Td}} = [\,V_{d1}\ V_{d2} \dots\ V_{dn}]^T, \boldsymbol{V_{Tq}} = \left[\,V_{q1}\ V_{q2} \dots\ V_{qn}\right]^T$$

$\boldsymbol{M} = diag(2H_i)$, $\boldsymbol{D} = diag(D_i)$
$\boldsymbol{T'_{do}} = diag(T'_{doi})$, $\boldsymbol{X_D} = diag(D_{di})$
$\boldsymbol{I_d} = [\, I_{d1} \;\; I_{d2} \cdots \;\; I_{dn}]^T$, $\boldsymbol{I_q} = [\, I_{q1} \;\; I_{q2} \cdots \;\; I_{qn}]^T$

$$\bar{I}_i = I_{di} + jI_{qi} \quad (19)$$

$$\bar{I}_i = \sum_{k=1}^{n} \bar{Y}_{ik} \left[E'_{qi} e^{j(\pi/2+\delta_{ik})} + (X_{qk} - X'_{dk}) I_{qk} e^{j\delta_{ik}} \right] \quad (20)$$

As we can see in (9), Y is reduced admittance matrices which contain only generators and UPFC buses. These reduced admittance and consequently above mentioned generators and UPFC currents represent all system power flow. Another important practical constraint which we have considered are limit of line thermal capacity which can be limited by applying limits of line ($\boldsymbol{S_{line,l}} \le \boldsymbol{S_{max,l}}$, $\boldsymbol{l = 1{:}\,n_{line}}$). While in each every iteration we compute admittances, currents and powers. While we adjusting UPFC parameters with considering these lines power limits, we modify adjusted UPFC parameters.

Above equations can be rewritten in following matrices form:

$$\dot{\boldsymbol{\delta}} = \omega_b(\boldsymbol{\omega} - 1) \quad (21)$$
$$\dot{\boldsymbol{\omega}} = \mathbf{M}^{-1}(\mathbf{T_m} - \mathbf{T_e} - \mathbf{D}(\boldsymbol{\omega} - 1)) \quad (22)$$
$$\dot{\mathbf{E}}'_{\mathbf{q}} = \mathbf{T}'_{\mathbf{do}}(\mathbf{E_{fd}} - \mathbf{E}'_{\mathbf{q}} + (\mathbf{X_d} - \mathbf{X}'_{\mathbf{d}})\mathbf{I_d}) \quad (23)$$
$$\dot{\mathbf{E}}_{\mathbf{fd}} = (\mathbf{K_A}(\mathbf{V_{Ref}} - \mathbf{V_t}) - \mathbf{E_{fd}})/\mathbf{T_A} \quad (24)$$
$$\mathbf{T_e} = \mathbf{V_{td}}\mathbf{I_d} + \mathbf{V_Q}\mathbf{I_{tq}} \quad (25)$$
$$\boldsymbol{V_{td}} = \boldsymbol{X_q}\boldsymbol{I_q} \;,\; \boldsymbol{V_{tq}} = \boldsymbol{E'_q} - \boldsymbol{X'_d}\boldsymbol{I_d} \quad (26)$$

With linearization above equations:

$$\Delta\dot{\boldsymbol{\delta}} = \boldsymbol{\omega_b}\Delta\boldsymbol{\omega} \quad (27)$$
$$\Delta\dot{\boldsymbol{\omega}} = -\mathbf{M^{-1}}(\Delta\mathbf{T_e} + \mathbf{D}\Delta\boldsymbol{\omega}) \quad (28)$$
$$\Delta\dot{\mathbf{E}}'_{\mathbf{q}} = \mathbf{T}'^{-1}_{\mathbf{do}}(\Delta\mathbf{E_{fd}} - \Delta\mathbf{E}'_{\mathbf{q}} + (\mathbf{X_d} - \mathbf{X}'_{\mathbf{d}})\Delta\mathbf{I_d}) \quad (29)$$
$$\Delta\dot{\mathbf{E}}_{\mathbf{fd}} = (\mathbf{K_A}(\Delta\mathbf{V_{ref}} - \Delta\mathbf{V_t}) - \Delta\mathbf{E_{fd}})\mathbf{T_A^{-1}} \quad (30)$$
$$\Delta\mathbf{T_e} = \Delta\mathbf{I_q}\mathbf{E}'_{\mathbf{q0}} + \mathbf{I_{q0}}\Delta\mathbf{E}'_{\mathbf{q}} + \Delta\mathbf{I_q}(\mathbf{X_q} - \mathbf{X}'_{\mathbf{d}})\mathbf{I_{d0}} + \Delta\mathbf{I_d}(\mathbf{X_q} - \mathbf{X}'_{\mathbf{d}})\mathbf{I_{q0}} \quad (31)$$
$$\Delta\mathbf{V_{td}} = \mathbf{X_q}\Delta\mathbf{I_q} \;,\; \Delta\mathbf{V_{tq}} = \Delta\mathbf{E}'_{\mathbf{q}} - \mathbf{X}'_{\mathbf{d}}\Delta\mathbf{I_d} \quad (32)$$

Where:

$$\Delta\mathbf{T_e} = \mathbf{K_1}\Delta\boldsymbol{\delta} + \mathbf{K_2}\Delta\mathbf{E}'_{\mathbf{q}} + \mathbf{K_{pd}}\Delta\mathbf{V_{dc}} + \mathbf{K_{pe}}\Delta\mathbf{m_E} + \mathbf{K_{pde}}\Delta\boldsymbol{\delta}_{\mathbf{E}} + \mathbf{K_{pb}}\Delta\mathbf{m_B} + \mathbf{K_{pdb}}\Delta\boldsymbol{\delta}_{\mathbf{B}} \quad (33)$$
$$\Delta\mathbf{E_q} = \mathbf{K_4}\Delta\boldsymbol{\delta} + \mathbf{K_3}\Delta\mathbf{E}'_{\mathbf{q}} + \mathbf{K_{qd}}\Delta\mathbf{V_{dc}} + \mathbf{K_{qe}}\Delta\mathbf{m_E} + \mathbf{K_{qde}}\Delta\boldsymbol{\delta}_{\mathbf{E}} + \mathbf{K_{qb}}\Delta\mathbf{m_B} + \mathbf{K_{qdb}}\Delta\boldsymbol{\delta}_{\mathbf{B}} \quad (34)$$
$$\Delta\mathbf{V_t} = \mathbf{K_5}\Delta\boldsymbol{\delta} + \mathbf{K_6}\Delta\mathbf{E}'_{\mathbf{q}} + \mathbf{K_{vd}}\Delta\mathbf{V_{dc}} + \mathbf{K_{ve}}\Delta\mathbf{m_E} + \mathbf{K_{vde}}\Delta\boldsymbol{\delta}_{\mathbf{E}} + \mathbf{K_{vb}}\Delta\mathbf{m_B} + \mathbf{K_{vdb}}\Delta\boldsymbol{\delta}_{\mathbf{B}} \quad (35)$$
$$\Delta\mathbf{V_{dc}} = \mathbf{K_7}\Delta\boldsymbol{\delta} + \mathbf{K_8}\Delta\mathbf{E}'_{\mathbf{q}} + \mathbf{K_9}\Delta\mathbf{V_{dc}} + \mathbf{K_{ce}}\Delta\mathbf{m_E} + \mathbf{K_{c\delta\delta}}\Delta\boldsymbol{\delta}_{\mathbf{E}} + \mathbf{K_{cb}}\Delta\mathbf{m_B} + \mathbf{K_{c\delta\delta}}\Delta\boldsymbol{\delta}_{\mathbf{B}} \quad (36)$$

$$\begin{bmatrix} \Delta\dot{\boldsymbol{\delta}} \\ \Delta\dot{\boldsymbol{\omega}} \\ \Delta\dot{\mathbf{E}}'_{\mathbf{q}} \\ \Delta\dot{\mathbf{E}}_{\mathbf{fd}} \\ \Delta\dot{V}_{DC} \end{bmatrix} = \begin{bmatrix} \mathbf{0} & \omega_0\mathbf{I} & \mathbf{0} & \mathbf{0} & \mathbf{0} \\ -\mathbf{M}^{-1}\mathbf{K}_1 & -\mathbf{M}^{-1}\mathbf{D} & -\mathbf{M}^{-1}\mathbf{K}_2 & \mathbf{0} & -\mathbf{M}^{-1}\mathbf{K}_{\mathbf{pd}} \\ -\mathbf{T}'^{-1}_{\mathbf{do}}\mathbf{K}_4 & \mathbf{0} & -\mathbf{T}'^{-1}_{\mathbf{do}}\mathbf{K}_3 & \mathbf{T}'^{-1}_{\mathbf{do}} & -\mathbf{T}'^{-1}_{\mathbf{do}}\mathbf{K}_{\mathbf{qd}} \\ -\mathbf{T}_{\mathbf{A}}^{-1}\mathbf{K}_{\mathbf{A}}\mathbf{K}_5 & \mathbf{0} & -\mathbf{T}_{\mathbf{A}}^{-1}\mathbf{K}_{\mathbf{A}}\mathbf{K}_6 & \mathbf{T}_{\mathbf{A}}^{-1} & -\mathbf{T}_{\mathbf{A}}^{-1}\mathbf{K}_{\mathbf{A}}\mathbf{K}_{\mathbf{vd}} \\ \mathbf{K}_7 & \mathbf{0} & \mathbf{K}_8 & \mathbf{0} & -\mathbf{K}_9 \end{bmatrix} \begin{bmatrix} \Delta\boldsymbol{\delta} \\ \Delta\boldsymbol{\omega} \\ \Delta\mathbf{E}'_{\mathbf{q}} \\ \Delta\mathbf{E}_{\mathbf{fd}} \\ \Delta V_{DC} \end{bmatrix}$$
$$+ \begin{bmatrix} \mathbf{0} & \mathbf{0} & \mathbf{0} & \mathbf{0} \\ -\mathbf{M}^{-1}\mathbf{K}_{\mathbf{pe}} & -\mathbf{M}^{-1}\mathbf{K}_{\mathbf{pde}} & -\mathbf{M}^{-1}\mathbf{K}_{\mathbf{pb}} & -\mathbf{M}^{-1}\mathbf{K}_{\mathbf{pdb}} \\ -\mathbf{T}'^{-1}_{\mathbf{do}}\mathbf{K}_{\mathbf{qe}} & -\mathbf{T}'^{-1}_{\mathbf{do}}\mathbf{K}_{\mathbf{qde}} & -\mathbf{T}'^{-1}_{\mathbf{do}}\mathbf{K}_{\mathbf{qb}} & -\mathbf{T}'^{-1}_{\mathbf{do}}\mathbf{K}_{\mathbf{qdb}} \\ -\mathbf{T}_{\mathbf{A}}^{-1}\mathbf{K}_{\mathbf{A}}\mathbf{K}_5 & -\mathbf{T}_{\mathbf{A}}^{-1}\mathbf{K}_{\mathbf{A}}\mathbf{K}_{\mathbf{vde}} & -\mathbf{T}_{\mathbf{A}}^{-1}\mathbf{K}_{\mathbf{A}}\mathbf{K}_{\mathbf{vb}} & -\mathbf{T}_{\mathbf{A}}^{-1}\mathbf{K}_{\mathbf{A}}\mathbf{K}_{\mathbf{vdb}} \\ K_{ce} & K_{cde} & K_{cb} & K_{cdb} \end{bmatrix} \begin{bmatrix} \Delta m_E \\ \Delta\delta_E \\ \Delta m_B \\ \Delta\delta_B \end{bmatrix} \quad (37)$$

Detailed values calculation of K coefficients can be find in [2]. As we can see the above equation is the standard form of linear system as below:

$$\Delta\dot{\boldsymbol{X}} = \boldsymbol{A}\Delta\boldsymbol{X} + \boldsymbol{B}\Delta\boldsymbol{U} \quad (38)$$

This matrices equation is suitable for classical linear control and numerical solving the system equations as well as controllability analysis such as Eigen values related techniques.

7. System simulation

7.1. Implementation algorithm

We have applied this simulation method to several power systems and we bring results of two of them here, first one is 39 bus new England power network and second one is IEEE 9 bus test system. For small signal analysis the sampling time selected 0.1 msec thus frequency of two UPFC inverters parameters updating is 10 khz which have compliance with nowadays switches speeds. In both two cases a power system Stabilizer (PSS) has used only for the generator which is installed on the slack bus. This study can be briefly described in the following flowchart:

i. Reading power system and UPFC data;
ii. Load flow running with considering practical limits and obtaining steady state operating point data of system and machines;
iii. Using operating point data to calculate UPFC parameters;
iv. Running load flow with UPFC installed regarding constraints and then obtaining new parameters values of system, machines and UPFC;
v. Computing linearized equations format of whole system using previous step data and system Eigen values;
vi. Calculating POD optimized parameters using PSO;
vii. Small signal equations solving with all four adjusted PI basic controllers of UPFC and adjusting UPFC four parameters in every each iteration in all time intervals consisting before, during and after fault occurrence;
viii. Considering practical constraints of lines and UPFC ratings in each every iteration and modifying UPFC parameters and obtained powers if needed;
ix. Modifying POD parameters to new optimized values if needed in some iteration.

7.2. The 39-Bus Power system simulation results

Figure 4 shows the studied power system which is 10-machine 39-bus New England network. In this study, a MATLAB program to simulate the model has used. The result of load flow implementation is used to find UPFC placement to improve voltage profile and load flow of power system.

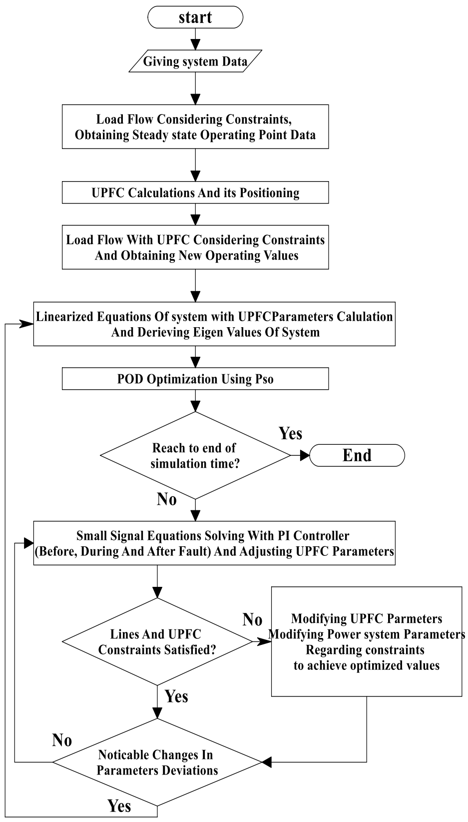

Fig. 3. Flowchart of simulation and optimization

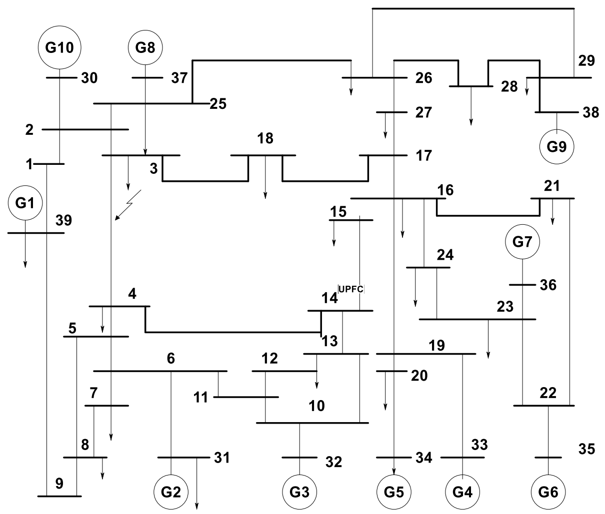

Fig. 4. New England power system network schematic single line

Within load flow solution the thermal limits of lines capacity considered. After UPFC insertion in power network the load flow executed again. It is shown that when UPFC is installed between two buses in the system, the active and reactive power loses are reduced. It is also has shown that not only the power losses are reduced, the voltage profile of the every bus improved after incorporate UPFC too.

For small signal and dynamic stability study we used UPFC dynamic model and interfacing with power system as described in 6.2. Linearized model of the multi-machine power system consisting in UPFC, has used to small signal analysis and damping oscillations studies. The power rating limits of UPFC and lines capacity limits have taken in to account during analysis. All four basic controller of UPFC considered. Eigen values and damping ratios of the linearized system derived and based on these values the PSO algorithm have used to optimize damping oscillations controller. Figure 5(a) demonstrates the Eigen values of the system with and without UPFC in complex plane. We can see some of Eigen values have a little more negative real part and smaller imaginary part. Figure 5(b) shows one machines speed and load angle before and after inserting UPFC which demonstrated the stabilizing impact of UPFC after earth fault occurrence.

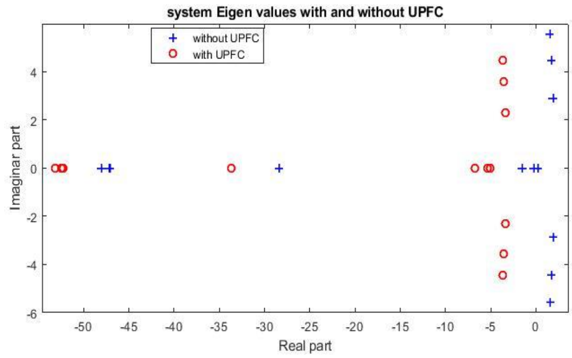

(a)

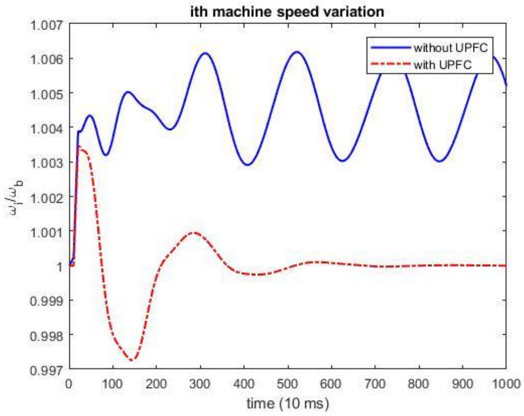

(b)

Fig. 5. System with and without UPFC comparison.(a)Eigen values.(b) machine no. 5 speed variation with and without UPFC in earth fault occurrence

To investigate enhancement of power system stability by a UPFC, we have studied results and responses of these two different scenarios: (1) three phase earth fault on the one of existing lines and (2) opening the circuit in one of the existing lines of power system. Removing time of both faults has selected enough small so we can use small signal analysis and investigate dynamic stability. But in scenario 2 it may that in several conditions due to changing in network topology have changing in steady state operating point, and then previous parameters can’t be used thus should calculate new operating parameters of UPFC and system variables values.

For UPFC performance analyse, two cases have considered and applied to simulated system: (i) the practical constraints not applied; (ii) the practical constraints taken in to account.

7.2.1. Scenario 1: Short circuit fault

Three phase earth fault applied to line between bus 3 and 4 at 0.1 sec of simulation beginning and its duration to clear is less than 0.1 sec which is enough short for small signal analysis. Figure 6(a), shows the variation of four UPFC control parameters i.e. $\boldsymbol{m_E}$, $\boldsymbol{m_B}$, $\boldsymbol{\delta_E}$ and $\boldsymbol{\delta_B}$ and 6(b) four output linearized control variables: UPFC dc voltage, the UPFC installed or sending bus voltage magnitude, active and reactive power flow in UPFC installed line and 6(c) voltage of the bus which UPFC installed and 6(d) voltage of the bus which fault occurred in it and 6(e) active and 6(f) reactive power flow which have controlled by UPFC and 6(g) four machines speed variations before using UPFC and 6(h) same machines speed variations after using UPFC with three phase earth fault applied without considering practical constraints and limits.

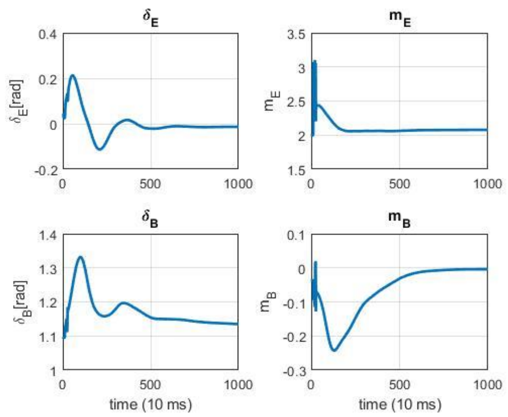

(a)

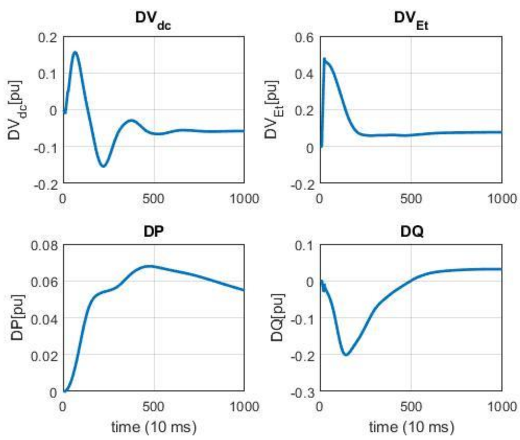

(b)

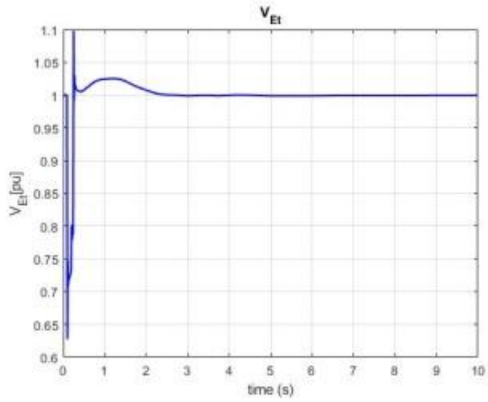

(c)

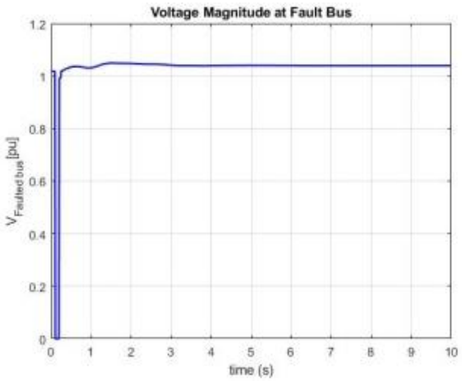

(d)

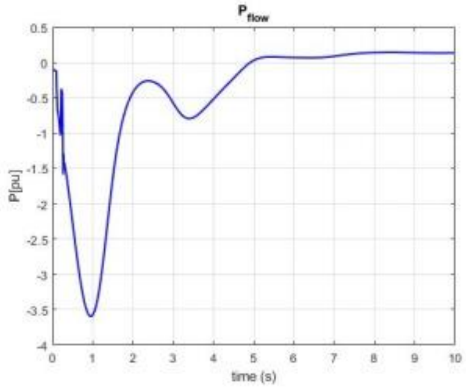

(e)

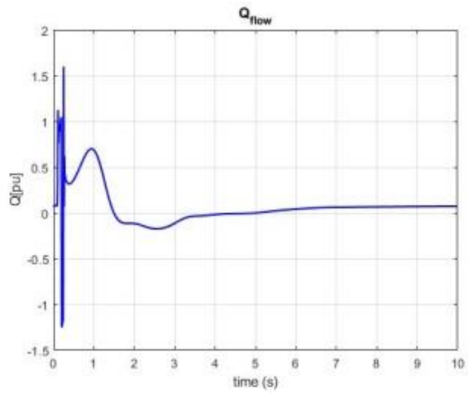

(f)

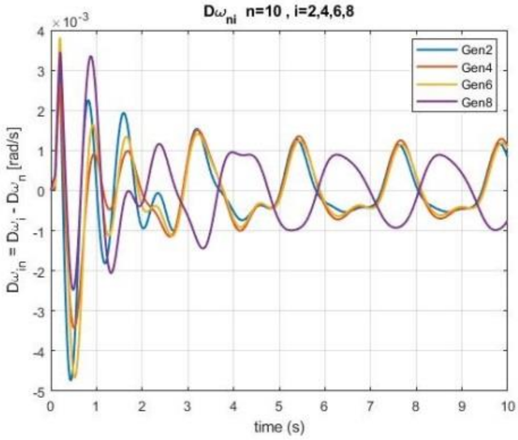

(g)

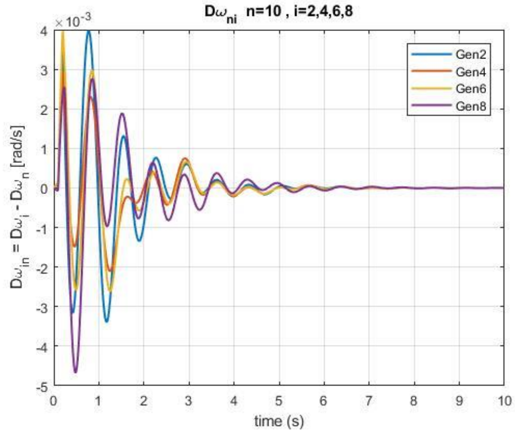

(h)

Fig.6. Damping effect of UPFC in three phase earth fault without considering practical limits in 39-Bus system.

Figure 7 shows the same parameters of figure 6 but with considering practical constraints and limits respectively.

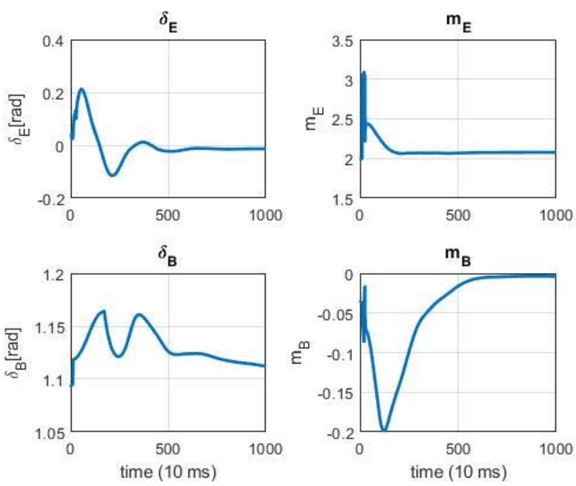

(a)

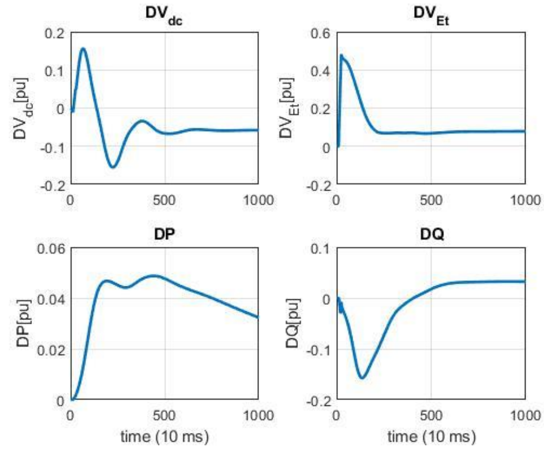

(b)

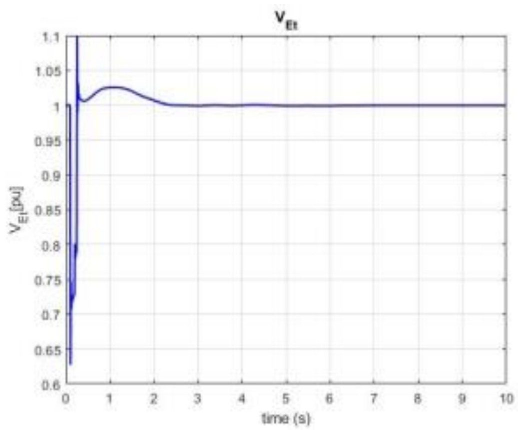

(c)

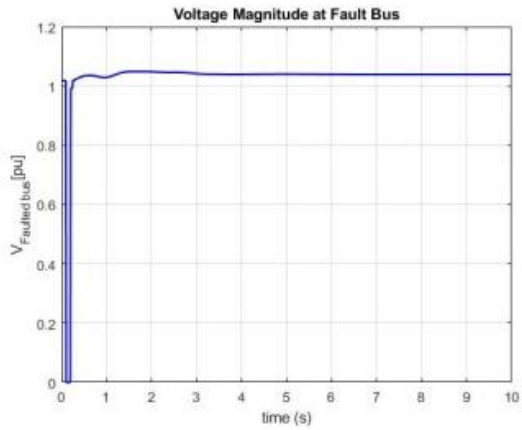

(d)

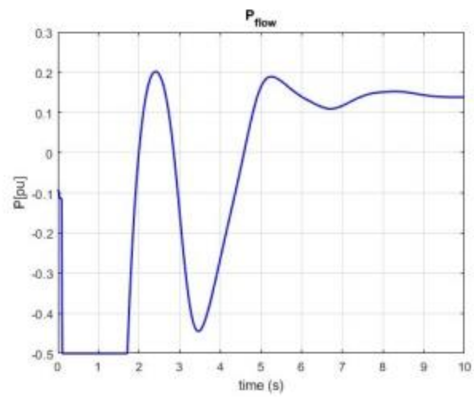

(e)

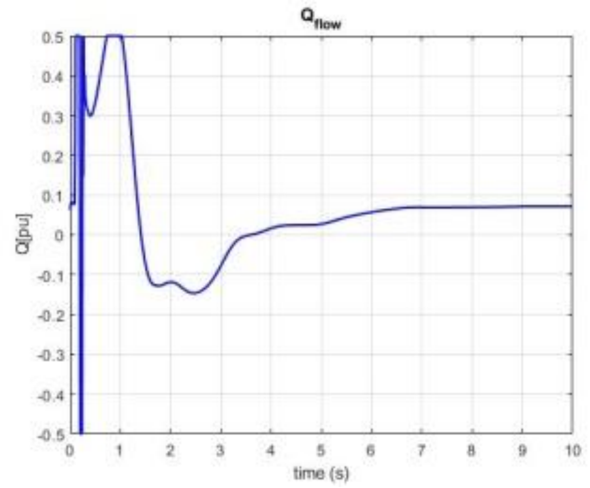

(f)

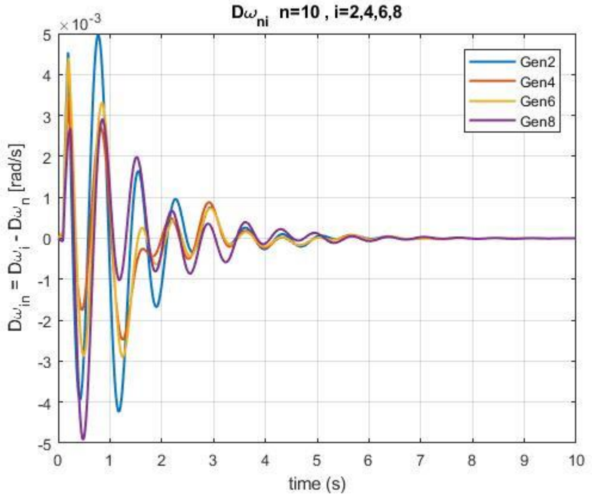

(g)

Fig. 7. Damping effect of UPFC in three phase earth fault with considering practical limits in 39-Bus system.

Figure 8 shows the effect of considering practical constraints in 39-Bus system. 8(a) demonstrate Active and reactive power flow in line which UPFC installed comparing result without considering constraint and with considering constraints and in 8(b) one machine speed and 8(c) one machine load angle in two condition , one with considering constraints and another without considering constraints. As we can see in two figures 6 and 7 and with compare them, and with more contrast in figure 8, it is observable that after fault the variation of active and reactive power which UPFC should control is too much and in real system we not permitted to have this rating with multiple time of base power rating. Because of applying these limit there are disturbances in UPFC controlled parameters but the results are more acceptable. And these limits consideration have not deteriorated stability and damping of oscillations and more or less lead to more stability.

7.2.2. Scenario 2: switch opening fault

The line switch between bus 13 and 14 has opened at 0.1 sec of simulation beginning and its duration is 0.1 sec too.

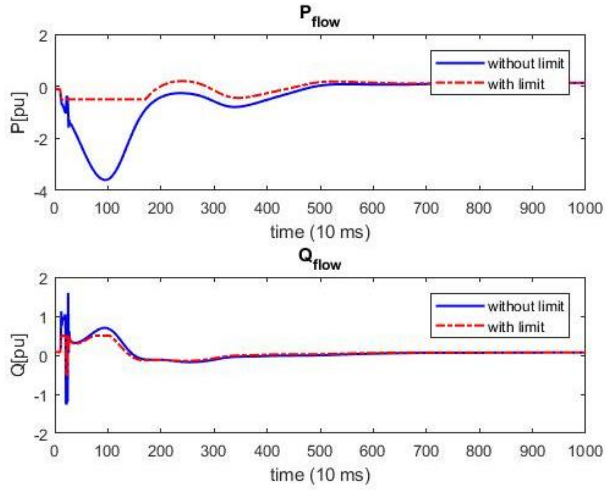

(a)

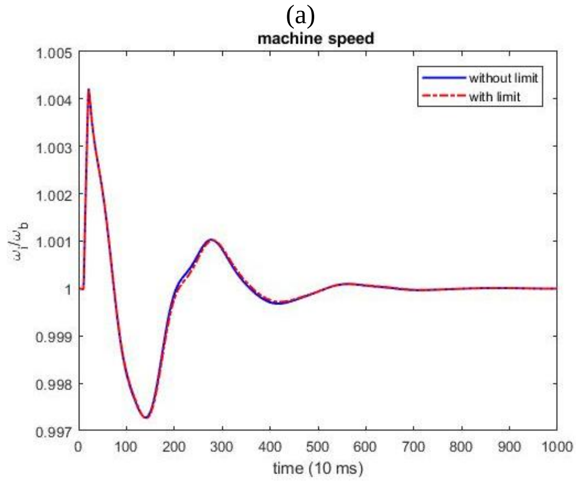

(b)

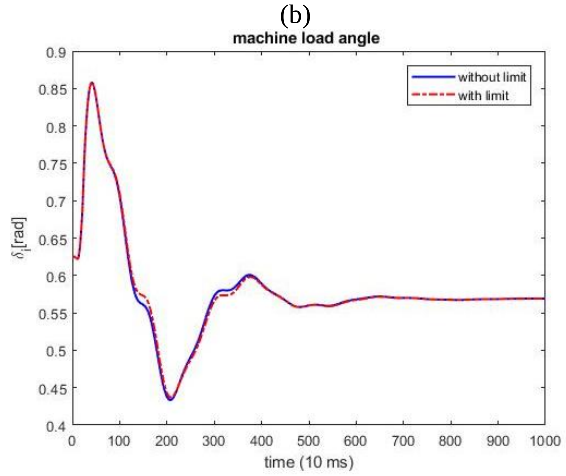

(c)

Fig. 8. Effect of practical constraints consideration in 39-Bus system

Figure 8 shows 9(a) voltage of the bus which UPFC installed and 9(b) voltage of the bus which the line which have opened had showed in 9(c) active and 9(d) reactive power flow which have controlled by UPFC and 9(e) 4 machines speed variation while UPFC not used and 9(f) four machines speed variations with UPFC and limits applied. As we can see in this scenario the operating point has changed. Then with controlled damping due to UPFC effect, parameters have changed to new values without instability.

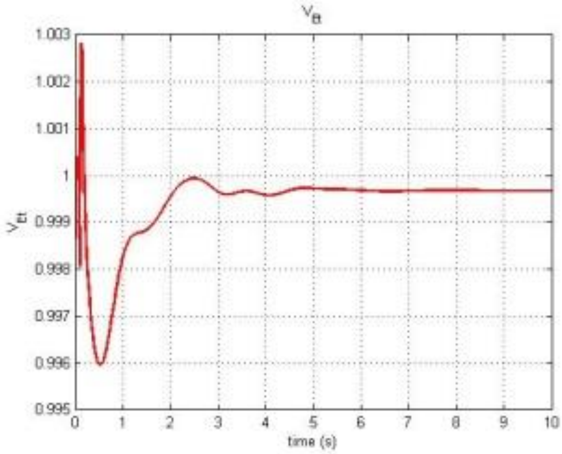

(a)

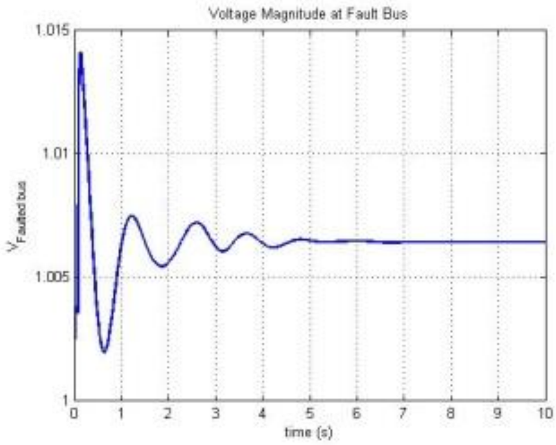

(b)

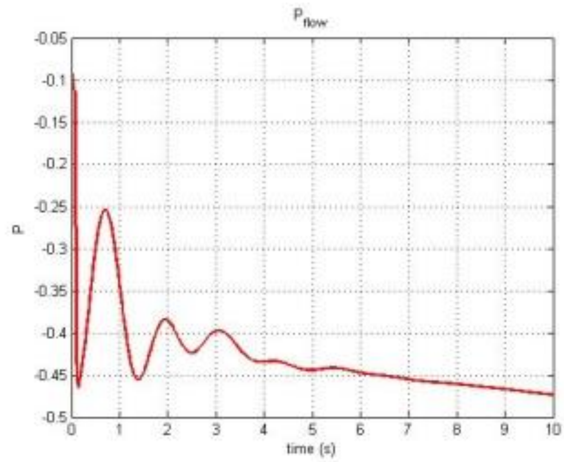

(c)

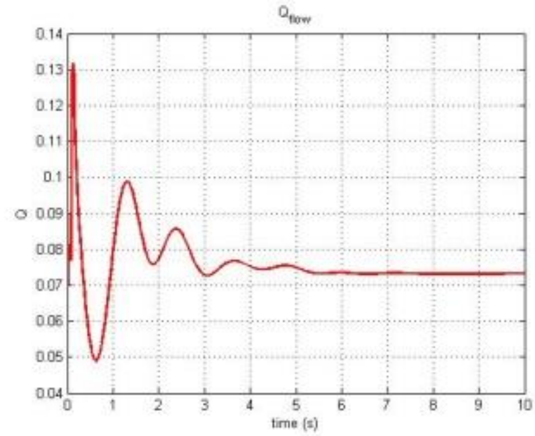

(d)

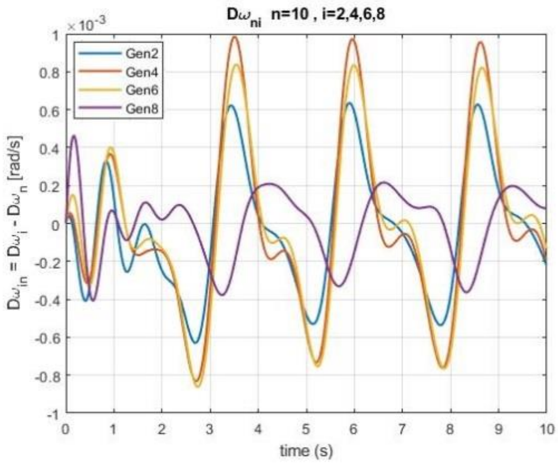

(e)

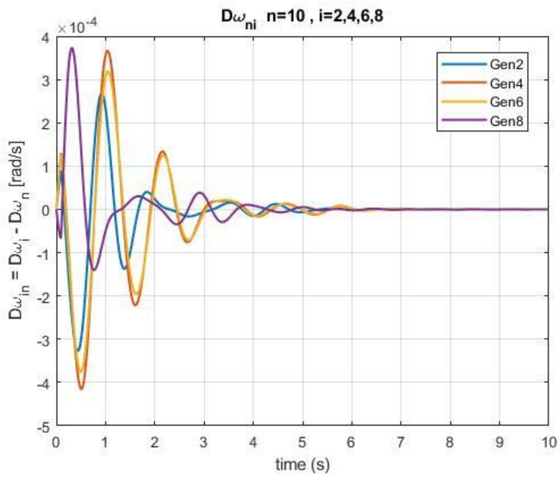

(f)

Fig. 9. Damping Effect of UPFC in line switch opening with considering practical limits in 39-Bus system.

7.3. The 9-Bus Power system simulation results

Figure 10 shows the 9 bus system with UPFC with short circuit fault applying in line between bus 2 and 3 in .1 sec after simulation and its duration is 0.1 sec. we compared the results of system response while considering practical constraints with them while hasn't considering those constraints.. As we can see in the figure 10(a), the practical constraints consideration leads to better and faster response of UPFC power flow.

In Figure 10(b) and (c) the speed and load angle of one of the machines have shown. And we can see that the practical limits consideration leads to different variation in speed and load angle of machines and has little affected the damping curve of them but hasn't deteriorate stability of machines and system.

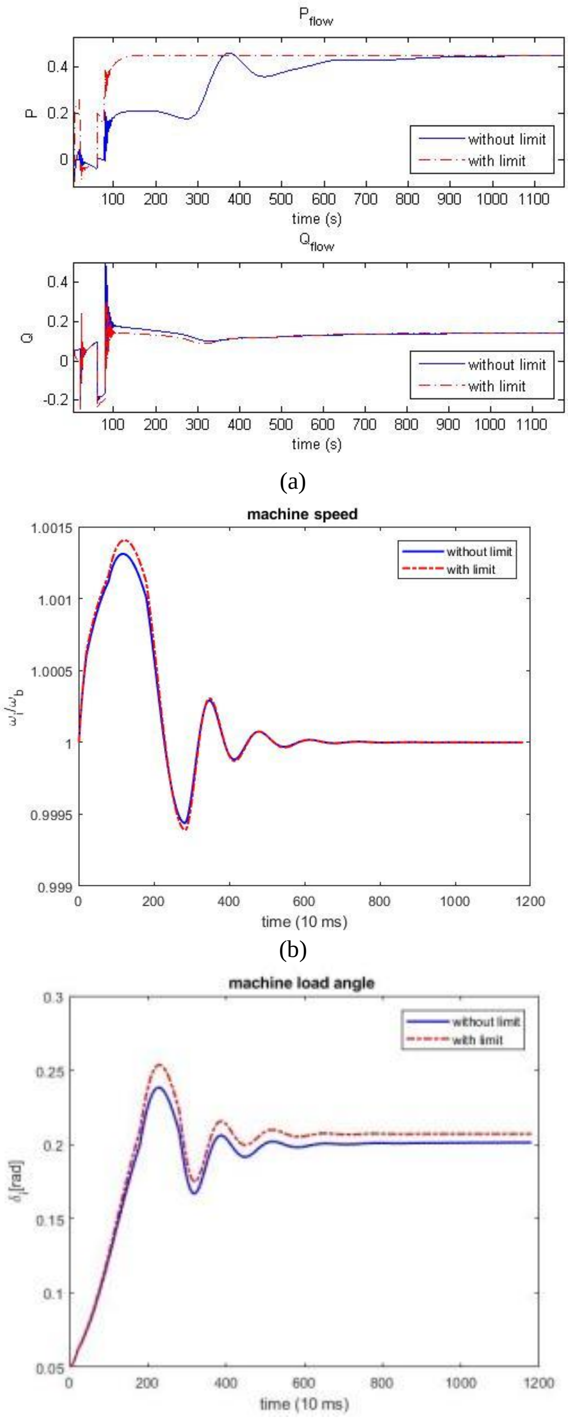

Fig. 10. Effect of practical constraints consideration in 9-Bus system

8. Conclusions

In this study, the power system with UPFC and its main and damping controls has modeled. All of four basic control and POD controller used simultaneously and sometimes we found the conflict between them during tuning of them but with compromising between them the conflict have acceptably reduced. We applied line transferring capacity thermal limits and UPFC active and reactive power ratings during load flow and small signal analyses. Applying practical constraints and limits affected the four parameters of UPFC adjusted values, so we have deviation in controlled parameters in particular active and reactive power damping trends. It is important that we hadn't any unsafe over/under shoots in electrical parameters which in real system not allowed and can't realize due to technical and economic aspects. The time of damping power and speed oscillations and settling may be little more while we applied those limits. In both two scenario the limits delayed the time of damping oscillations and omitted undesirable values, but in case of three-phase earth fault this effects is more considerable in compare with line opening. These limitation applying didn't deteriorate stability and Eigen values. This simple method even in some changing topologies leads to acceptable result in damping oscillation and stability analyses.

9. References

[1] M. Eslami, H. Shareef, M.R. Taha, M. Khajezadeh," Adaptive particle swarm optimization for simultaneous design of UPFC damping controllers", *ELSEVIER Electrical Power and Energy Systems,* vol. 57, pp. 116-128, 2014.

[2] M.R. Banaei, S.J. Seyed-Shenava, P. Farahbakhsh, "Dynamic stability enhancement of power system based on a typical unified power flow controllers using imperialist competitive algorithm*", Ain Shams Engineering Journal*, vol. 5, pp. 691–702, 2014.

[3] S.N. Dhurvey, V.K. Chandrakar," Performance comparison of UPFC in coordination with optimized POD and PSS on damping of power system oscillations", *WSEAS Transactions on Power Systems*, vol. 5, no. 3, pp. 287-299, 2008.

[4] A.J. Rahmaniar, R. Salman, G.A. Hamid K, J. Jalius, N. Jalinus, "Modeling and Simulation: A Comparison of LQR Control and Unified Power Flow Controller for Dynamic Stability Improvement", *International Journal of Engineering Research and Technology*, vol. 12, no. 7, pp. 1033-1038, 2019.

[5] M. Sebaa, O. Bekhechi, A. Chaker, "A Fuzzy Tuned Adaptive PI Controller Based UPFC to Improve Power Oscillations Damping in Multi Machine Power System", *International Review on Modelling and Simulations (I.RE.MO.S.)*, vol. 8, no. 3, pp. 307-314, June 2015.

[6] M.H. Ananda, M.R. Shivakumar, "Dynamic Power Oscillation Reduction using PSOA-PI in UPFC", *International Journal of Innovative Technology and Exploring Engineering (IJITEE)*, vol. 9, Issue 2, pp. 3046-3050, December 2019.

[7] B. K. Dubey, N.K. Singh, "Multimachine Power System Stability Enhancement with UPFC Using Linear QUADRATIC Regulator Techniques", *International Journal of Advanced Research in Engineering and Technology (IJARET)*, vol. 11, Issue 4, pp. 219-229, April 2020.

[8] N. Nahak, R. K. Mallick, S. P. Muni, "Stability Enhancement of Multi machine System by Improved GWO Optimized UPFC based controller", *International Journal of Pure and Applied Mathematics*, vol. 114, no. 9, pp 63-72, 2017.

[9] S. Abazari, O. Moradi, Improvement Damping Power System by using UPFC and Tuning Controller Parameter base on a New PSO Algorithm, *Tabriz Journal of*

Electrical Engineering, vol. 46, no. 1, pp. 1-11, spring 2016(in persian).
[10] K. Kumara, A.D. Srinivasan, "Comparison and Assessment of Conventional and Optimal Coordinated PSS and UPFC Damping Controller", *International Journal of Engineering and Advanced Technology (IJEAT)*, vol. 8, Issue 5, pp 389-393, June 2019.
[11] M. Ravindrababu, G. Saraswathi, K.R. Sudha, "Design of UPFC-PSS using Firefly Algorithm for Stability Improvement of Multi Machine System under Contingency", *Majlesi Journal of Electrical Engineering*, vol. 13, no. 2, pp21-39, June 2019.
[12] S. Choudhury, A. Satpathy, P. Rout, T. P. Dash, "Improvement of Dynamic Stability via Coordinated Design of PSS and UPFC in a Two Machine Power System Employing Cuckoo Search Optimization Technique", *International Journal of Recent Technology and Engineering (IJRTE)*, vol. 7, Issue 6, pp. 1922-1929, March 2019.
[13] S. Abazari, Z. Faramarzi, "Damping Improvement of Multi Machine Power System Oscillations by using UPFC Controller based Multi-input Nonlinear Backstopping Controller", *Tabriz Journal of Electrical Engineering*, Articles in Press, Accepted Manuscript, Available Online from 21 September 2020(in persian).
[14] H.F. Wang, "A unified model for the analysis of FACTS devices in damping power system oscillations – Part III: unified power flow controller', *IEEE Transation on Power Deliv*ery, vol. 15, no. 3, pp. 978–983, 2000.
[15] H.F. Wang, M. Jazaeri, Y.J. Cao, "Analysis of control conflict between UPFC multiple control functions and their interaction indicator", *International Journal of Control, Automation, and Systems*, vol. 3, no. 2(special edition), pp. 315-321, 2005.
[16] K.I. Prasanna, M.R. Shiva, "Development of a fuzzy control scheme with UPFC's for damping of oscillations in multi machine integrated power systems", *International Journal of Engineering Research and Applications (IJERA)*, vol. 1, no. 2, pp. 230-234, 2011.
[17] A.K. Baliarsingh, S. Panda, A.K. Mohanty, C. Ardil, "UPFC supplementary control design using real-coded genetic algorithm for damping low frequency oscillation in power system", *International Journal of Electrical, Robotics, Electronics and Communications Engineering*, vol. 7,no. 4, pp. 261-271, 2013.
[18] Y. Shi, R. Eberhart, "A modified particle swarm optimizer", IEEE international conference on evolutionary computation proceedings, 1998, Anchorage, AK, USA, pp. 69–73.
[19] A. Nabavi-Niaki, M.R. Iravani, "Steady-state and dynamic models of unified power flow controller for power system studies", *IEEE Transactions on Power Sys*tem, vol. 11, no. 4, pp. 1937-1950, 1996.
[20] P. Kundur, "Power System Stability and Control", Electric Power Research Institute, Power System Engineering Series, McGraw-Hill, New York, 1994.

Appendix:
UPFC used Data:

In IEEE 9-Bus system: UPFC Rating=0.5 pu, xE=0.05 pu, xB=0.05 pu, Cdc=1 pu, Sb=100MW.

In 39-bus New England network: UPFC Rating=1.9 pu, xE= 0.0725 pu, xB=0.0725 pu, CDC=1 pu, Sb=100MW.